energies

MDPI

Article

Component Sizing of an Isolated Networked Hybrid Microgrid Based on Operating Reserve Analysis

Navid Salehi, Herminio Martínez-García * and Guillermo Velasco-Quesada

Electronic Engineering Department, Universitat Politècnica de Catalunya–BarcelonaTech (UPC), 08019 Barcelona, Spain

* Correspondence: herminio.martinez@upc.edu

Abstract: The power-sharing possibility amongst microgrids (MGs) in networked microgrids (NMGs) offers multiple profits to the NMG by employing an applicable energy management system. An efficient energy management system can provide an adequate compromise in terms of the component sizing of NMGs through MG collaboration. This paper proposes a procedure to size the component for an isolated networked hybrid microgrid. The proposed design procedure relies on the optimum operation of individual MGs. The defined Reduced Factor (RF) identifies the possible size reduction for the dispatchable components, such as diesel generators and the energy storage system of each MG. The introduced RF is based on the operating reserve evaluation obtained from the optimal operation of individual MGs and the correlation between load profiles. Eventually, the simulation and practical results of a networked hybrid MG consisting of three MGs are presented to verify the proposed component sizing procedure. The practical results verify the theoretical expectations. The results show that NPC and capital costs are reduced up to 13% and 17%, respectively.

Keywords: networked hybrid microgrid; operating reserve; peak load; component sizing; optimization

Citation: Salehi, N.; Martínez-García, H.; Velasco-Quesada, G. Component Sizing of an Isolated Networked Hybrid Microgrid Based on Operating Reserve Analysis. *Energies* **2022**, *15*, 6259. https://doi.org/10.3390/en15176259

Academic Editor: Dimitrios Katsaprakakis

Received: 14 July 2022
Accepted: 15 August 2022
Published: 27 August 2022

1. Introduction

Conventional power systems have adopted microgrids (MGs) to address concerns about fossil fuel source depletion, environmental pollution, and climate change. Distributed energy resources (DERs) in an MG can consist of conventional power generators, such as diesel generators (DGs), or they can be integrated with renewable energy sources (RESs), such as photovoltaic (PV) and wind turbine (WT), as a hybrid MG (HMG). MGs propose valuable features to the power system, such as improving the operation and stability of the distributed system, reducing transmission line losses, and efficient harvesting of REs. These features can be obtained in both grid-connected and stand-alone MGs. However, the stand-alone operation mode in MGs is more delicate to provide the system's power balance due to the intermittency and uncertainty of RE sources (RESs). To this end, energy storage systems (ESSs), such as batteries and fuel cells, are inevitably utilized in the MGs. The ESS makes the system controllable to effectively manage the energy to supply the demand load. Therefore, the energy management system (EMS) is the other vital part of MGs, not only to provide the stability of the system but also to optimize the operation of the MG [1].

Accordingly, the configuration and the size of the components of the power generation units in an MG have attracted the attention of researchers in this industry to propose effective solutions for MGs. In [2], a multi-objective optimization problem was defined for an HMG to obtain the optimum size of the components. The net present cost (NPC), emission penalty cost, and CO2 released quantity are three objective functions defined as a minimization problem. Moreover, the results from three multi-objective optimization—MOPSO, PESA-II, and SPEA-II—were analyzed to achieve the best solution to fulfill the objectives. A similar study was conducted in [3] to optimize the size of HMG components. The multi-objective self-adaptive differential evolution (MOSaDE) was assigned to the

optimization approach to propose the optimal HMG configuration. The loss-of-power supply probability (LPSP), the cost of electricity (COE), and the renewable factor are the three objective functions of the optimization problem that are restricted with HMG cost and reliability. The paper presented the optimally sized HMG components considering the load supply with a minimum energy cost and high reliability. Additionally, an optimal sizing methodology for an MG consists of a stand-alone photovoltaic system (SAPV), and the battery were studied in [4]. A mutation adaptive differential evolution (MADE) optimization algorithm was performed to optimize the configuration of the off-grid MG. The loss-of-load probability (LLP), levelized cost of energy (LCE), and life-cycle cost (LCC) are three objective functions that are normalized, weighted, and aggregated as a single objective for the optimization algorithm. In [5], the other HMG consists of renewable energies, and conventional energy sources were studied by considering the load uncertainty. To obtain the optimal configuration for the HMG, a decomposition-based multi-objective evolutionary algorithm (MOEA/D) was applied to minimize the LPSP and COE as the objective functions. In [6], the inconstancy and unpredictability of solar radiation were considered in the proposed hybrid optimization method of a SAPV/battery MG to optimize the configuration and size of the system.

Furthermore, some software tools have been introduced by several companies to plan the MG optimally. HOMER, RETScreen, H2RES, DER-CAM, and MARKAL/TIMES are several practical applications in MG design planning [7,8]. HOMER is widely used in MG applications to design the optimal MG consisting of renewable and non-renewable energy sources with different storage systems in grid-connected and isolation operation modes. In HOMER, the optimization procedure evaluates all possible configurations of energy generator units to meet the load. The simulation in HOMER carries out for a long time according to the cost function of the MG components. The results in HOMER present the most economic configurations with the lowest net total cost (NTC). In [9], HOMER develops an optimized grid-connected MG with PV and battery configuration. This study investigates the effect of the upsurge of grid failure frequency, and grid mean repair on the power price. Additionally, other studies have been conducted using HOMER to design HMG in remote areas, select and size power generators in rural MGs, and plan the micro-source generators to accommodate the high demand of RESs and environment policy [10,11]. RETScreen is more used to analyze the MG economically rather than operationally. The RETScreen can also be applicable for on-grid and off-grid MGs. The changes in parameters in RETScreen can provide a comparative analysis for the system under study considering the climate condition, RES availability, and load requirements [12]. The H2RES is also a balancing simulation tool that can effectively be used to design an MG integrated with RE. This tool checks the energy balance of the system hourly, considering the economic restriction [13]. The DER-CAM optimization is a customer-based model tool that monitors demand-side management and time-of-use under control by scheduling the DERs [14,15]. The MARKEL/TIMES energy system model can be applied to analyze the MG system as an energy sector. This tool evaluates the energy system in various time slices by considering the energy markets with a different objective function to obtain the least cost production units [16].

Recently, the concept of networked MG (NMG) has emerged to enhance the successful achievements of IMG. In NMGs, several MGs coordinate cooperatively to achieve the following goals:

- Increasing the reliability of the system due to increasing the possibility of power sharing and avoiding imbalanced power situation;
- Increasing the penetration ratio of REs into the MGs;
- Suppressing the uncertainties related to the RES employing the energy management system (EMS);
- Energy trading and ancillary service management.

On the other hand, the control strategies in NMGs are more complicated than in IMGs. In recent years, several control strategies have been introduced by researchers to control the

NMG effectively. Centralized, decentralized, hybrid, and distributed are some of the most prominent control strategies in NMGs. Each control strategy has its pros and cons, which, in several studies, are comprehensively surveyed [17,18]. However, briefly explained, in a centralized control scheme, all the MGs are controlled by a central controller; therefore, knowing the status of all MGs to analyze the system is mandatory. This control method is efficient and accurate. However, the enormous computing burden and dependency of the system on the central controller are the disadvantages of this method. In a decentralized control strategy, each MG controls separately to overcome the afore-mentioned drawbacks in the centralized method. However, optimizing the system without knowing other MGs' information reduces the system's efficiency. Therefore, in a hybrid strategy, the advantages of both centralized and decentralized methods are exploited. However, this method still suffers from the dependency on the central controller and the possibility of global failure in the system by any probable fault in the central controller. Finally, distributed control strategies have recently drawn more attention to increase the speed of analysis; meanwhile, the system's reliability increased as well.

In NHM, due to the possibility of power sharing amongst MGs, it is expected that the size of the components can be reduced effectively without significantly affecting the system's reliability. In [19], a three-level planning model for optimal sizing of NMG considering resilience and cost was proposed. An adaptive genetic algorithm was utilized for the normal sizing problem in the first level. However, load profile uncertainty and contingency for load shedding and a trade-off between cost and resilience were evaluated in the second and third levels, respectively. In [20], an optimal design of a hybrid distributed generation system to enhance the load and system reliability is conducted. The optimal sizing of the RE system considering electricity market interaction and reliability is presented in [21]. High renewables penetration considering demand response is investigated in [22] by proposing an optimal sizing and siting of smart MG components.

This paper proposes an optimal sizing components methodology for an isolated networked hybrid MG. The design procedure is based on IMG optimization. Consequently, according to the optimized operation of each IMG, a reduced factor (RF) identifies the possible component size reduction of each MG. This paper is organized as follows: In Section 2, the proposed NHMG configuration with RE and non-RE sources and load profiles are presented. Then, the optimal sizing of HIMG is investigated. To this end, HOMER is used to obtain the most economical configuration and component size for each IMG according to the energy sources and practical restrictions of the energy generator units. To evaluate the operation of the MGs, the optimal operation of each IMG is calculated for 24 h by considering the defined energy management algorithm. The RF calculation is conducted at the end of this section. In Section 3, the proposed sizing component algorithm is evaluated, and the simulation results will be presented in order to calculate the RF for each IMG. In Section 4, the verification of the proposed algorithm for an NHMG is analyzed according to the simulation and practical results. Finally, in Section 5, the conclusion of the paper is presented.

2. Proposed Optimal Sizing Procedure of an NHMG

The networked hybrid microgrid (NHMG), consisting of PV and WT with battery storage and DG, is investigated in this section. Figure 1 shows an HNMG of three MGs involving two residential and one industrial consumer. The MGs can exchange energy to provide a reliable operation to meet the loads according to the defined strategy. The load profiles are shown in Figure 4. As can be seen, the load profile of two residential consumers have the same pattern but with a different scale, and the load profile of industrial consumer has a different pattern. In this paper, to optimize the size of the components in HNMG, an algorithm is proposed. In this algorithm, the optimal design of the HNMG is based on the optimal design of each IMG. Figure 2 represents the proposed algorithm.

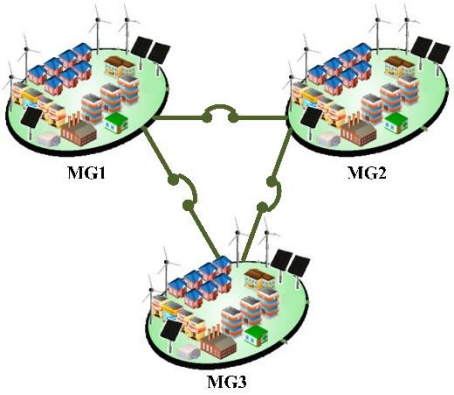

Figure 1. NMG consists of three residential MG and one industrial MG.

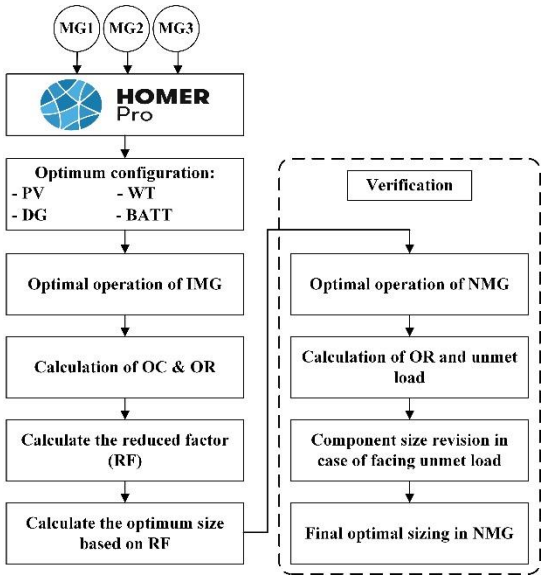

Figure 2. Proposed algorithm of NMG optimal sizing.

The optimal component size for each MG was obtained by HOMER Pro to evaluate the most economical configuration of potential candidate energy resources. According to the optimal sizing of each MG, power management was applied to the MGs to control the power production of dispatchable units, i.e., battery and DG. Moreover, the practical constraints and renewable energy intermittency were taken into consideration. Accordingly, the operating capacity (OC) and operating reserve (OR) of the individual MGs can be obtained. The calculation of OC and OR are essential due to the dependency of the optimization algorithm on these values. The OC and OR are defined as follows:

- Operating capacity (OC): the maximum amount of electrical generation capacity that is operating or is able to be produced at a moment's notice.
- Operating reserve (OR): the surplus operating capacity that can instantly respond to a sudden increase in the electric load or a sudden decrease in the renewable power output.

Peak load (PL) is an important factor with a significant impact on the component sizing in MGs. Demand-side management (DSM), integration of ESSs, and integration of electric vehicles (EVs) to the grid are considered as three methods in recent research as a solution for peak load shaving [23]. However, power sharing amongst MGs in NMGs results in the possibility of providing PL demand with the OR of adjacent MGs. The PLs and ORs are considered two main factors of MGs to define a reduced factor (RF) by the proposed algorithm in this paper. The RF represents the amount of energy that can be reduced when the MGs collaborate as an NMG. Consequently, the RFs assess the size of

dispatchable components while avoiding the reliability compromise due to OR reduction. Renewable energies exploit their maximum power due to utilizing maximum power point tracking (MPPT) to optimize the harvested energy.

2.1. Optimal Sizing of Hybrid Individual MGs

In order to obtain the optimal size of HIMGs, the power output and the cost function of power generator units have to be considered for each time step to supply the load in the most economical manner. The more precise power output model and cost function equations result in more accurate calculations. Tables 1 and 2 present the most well-known equations for power generation units and their cost functions. By considering the power output in Table 1, the optimization problem can be defined as:

$$\min CF = \{CF(PV) + CF(WT) + CF(DG) + CF(BAT)\} \quad (1)$$

Subject to:

$$P_{PV}(t) + P_{WT}(t) + P_{DG}(t) + P_{BAT}(t) = P_{Laod}(t) \quad (2)$$

Equations (1) and (2) expressed that the total cost functions of generation units must be minimized considering the power balance of the system in each time step. Although only the power balance is stated as a constraint in this optimization problem, practically more constraints such as upper and lower limits for power generation units or battery SoC can be defined for this problem.

Table 1. Power output and cost function of power generation units in a HIMG.

Gen Unit	Ref.	Power Output	Cost Function
PV	[3,24]	$P_{pv}(t) = P_{N-pv} \times \frac{G(t)}{G_{ref}} \times \left[1 + K_t\left((T_{amb} + (0.0256 \times G)) - T_{ref}\right)\right]$	$C_{PV} = \alpha I_{pv}^{P} P_{N-pv} + G_{pv}^{E} P_{N-pv}$
WT	[5,24]	$P_{wt}(t) = \begin{cases} 0 & V < V_{cut-in}, V > V_{cut-in} \\ V^3(t)\left(\frac{P_r}{V_r^3 - V_{cut-in}^3}\right) - P_r\left(\frac{V_{cut-in}^3}{V_r^3 - V_{cut-in}^3}\right) & V_{cut-in} \le V < V_{rated} \\ P_r & V_{rated} \le V \le V_{cut-out} \end{cases}$	$C_{WT} = \alpha I_{pv}^{P} P_{N-r} + G_{wt}^{E} P_{N-r}$
DG	[3]	$P_{DG}(t) = \frac{q(t) - bP_r}{a}$	$C_{DG} = A + B \times P_{DG} + C \times P_{DG}^2$
BAT	[2]	$P_{BATT}(T) = \frac{v}{T} \frac{E_L.AD}{DOD.\eta_{inv}.\eta_b}$	$C_{BAT} = \gamma + \xi \times P_{N-BAT}$

Table 2. Parameter definitions in Table 1.

Parameter	Description	Parameter	Description
P_{pv}	output power of PV	a, b	fuel consumption coefficients (L/kW) [3]
$P_{N\text{-}pv}$	rated power under reference conditions	E_L	load power
G	solar radiation (W/m^2)	AD	autonomy days (typically 3–5 days)
G_{ref}	reference solar radiation (W/m^2)	DOD	depth of discharge
T_{ref}	25 °C	η_{inv}	inverter efficiencies
K_t	-3.7×10^{-3} (1/°C)	η_b	battery efficiencies
P_{wt}	output power of WT	$A = r/[1 - (1 + r)^{-N}]$	investment annuitization coefficient
P_r	rated power	r	interest rate
V_r	rated wind speed	N	investment lifetime
$V_{cut\text{-}in}$	cut-in wind speed	I^P	investment costs
$V_{cut\text{-}out}$	cut-out wind speed	G^E	O&M cost for solar and wind generation [24]
$q(t)$	fuel consumption (L/h)	A, B, C	generator coefficients
$P(t)$	generated power (kW)	γ, ξ	coefficients to linearize the cost function of batteries according to the capital cost and operation cost of batteries

HOMER Pro can effectively size the MG components consisting of the conventional power generation such as DGs, REs such as solar and wind energy, and energy storage systems (ESSs) such as batteries and fuel cells both in the grid-connected and stand-alone modes. HOMER analyzes all feasible solutions to meet the load and sorts them from the most economical configuration to the least one. To this end, the potential candidates for power generation have to be defined, and the cost of each unit must be determined. The cost in HOMER consists of capital cost, replacement cost, and operation and maintenance (O&M) cost. The capital cost is the initial investment to provide the power generation units. The replacement cost is the cost of replacing the units at the end of their lifetime. Additionally, the O&M cost is referred to as annual operation and maintenance cost. Moreover, cycling charging (CC) and load following (LF) are the two most common strategies in HOMER to control the power dispatch in the MG. The CC dispatch strategy is more economical when the RE generation consists of a lower portion of the total required energy. In this case, the dispatchable generators, such as DG, operate at full output power, and surplus energy charges the storage systems, such as batteries. On the other hand, in the LF strategy, the dispatchable units only produce the required power to supply the unmet load by REs, and REs can charge the storage systems if extra power is produced. The practical constraints for each power generation unit, operating reserve, and emission and environmental effects can be defined in HOMER effectively.

Table 3 represents the optimum design of the three MGs considering the load profiles in Figure 2 by HOMER Pro. The considered MGs are situated in the geographical coordinates of 41°23′04″ N, 02°10′27″ E (Barcelona City). The solar, wind, and temperature resources were loaded from NASA Prediction of Worldwide Energy Resources, and Table 4 presents the relevant costs. In order to increase the reliability of the MGs, the operating reserve for solar and wind power output and load in each current time step was considered and presented as the constraints in Table 4. Because forecasting solar radiation is more reliable than wind profile, the operating reserve for WT is usually greater than PV.

Table 3. HIMG optimal design by HOMER.

	PV (kW)	WT (kW)	DG (kW)	BAT (kWh)	Converter (kW)	Dispatch	NPC ($)	Unmet Electric Load	Capacity Shortage
MG1	6.5	2	6.8	29	2.95	LF	80,980	0	0
MG2	8.31	3	9.1	38	4.03	LF	107,774	0	0
MG3	16.8	4	15	57	9.71	CC	234,924	0	0

Table 4. Economical and constraints parameters.

Gen Unit	Parameter	Value	Unit	Gen Unit	Parameter	Value	Unit
PV	Capital	2500	USD/kW	**WT**	Capital	3000	USD/kW
	Replacement	2500	USD/kW		Replacement	3000	USD/kW
	O&M	10	USD/kW/year		O&M	30	USD/kW/year
	Derating Factor	80	%		Hub Height	17	m
	Lifetime	25	year		Lifetime	20	year
DG	Capital	500	USD/kW	**BAT**	Capital	300	USD/kW
	Replacement	500	USD/kW		Replacement	300	USD/kW
	O&M	0.03	USD/kW/year		O&M	10	USD/kW/year
	Fuel Price	1	USD/L		Min SOC	40	-
	Lifetime	15 k	hour		Lifetime	10	year
CONVERTER	Capital	300	USD/kW	**CONSTRAINTS**	Load in current time step		10%
	Replacement	300	USD/kW		Annual peak load		0
	O&M	0	USD/kW/year		Solar power output		20%
	Lifetime	15	year		Wind power output		50%

2.2. Optimal Operation of HIMGs

According to the obtained optimal size of HIMG, the optimal operation of the MGs over 24 h was performed to calculate the produced energy (PE) and OR of each power generator unit in the MGs. To this end, the cost functions in Table 1 were used. However, to achieve the maximum power from REs, it was supposed that a maximum power point tracking (MPPT) was applied to the PV and WT. Therefore, the DG and battery power as the decision variables and battery SoC as the state variable were defined for the optimizer in order to determine the most economical operation for MGs. Consequently, the optimization problem can be defined as cost function (CF) minimization of the total sum of DG and BAT:

$$\min\{CF(DG) + CF(BAT)\} \tag{3}$$

Subject to:

$$P_{DG}(t) + P_{BAT}(t) = P_{Load}(t) - P_{PV}(t) - P_{WT}(t) \tag{4}$$

$$P_{DG\min} \leq P_{DG} \leq P_{DG\max} \tag{5}$$

$$0 \leq P_{BAT} \leq P_{BAT\max} \tag{6}$$

$$So\ C_{\min} \leq So\ C(t) \leq So\ C_{\max} \tag{7}$$

where the SoC of the battery can calculated by:

$$So\ C(t + \Delta t) = So\ C(t) + \frac{\Delta t}{C_{BAT}} P(t) \tag{8}$$

In (8), the power $P(t)$ can be positive or negative regarding the discharging or charging state of the battery.

To obtain the optimal operation for each MG, a power management unit has to be applied to the system. Figure 3 represents the power management in this paper.

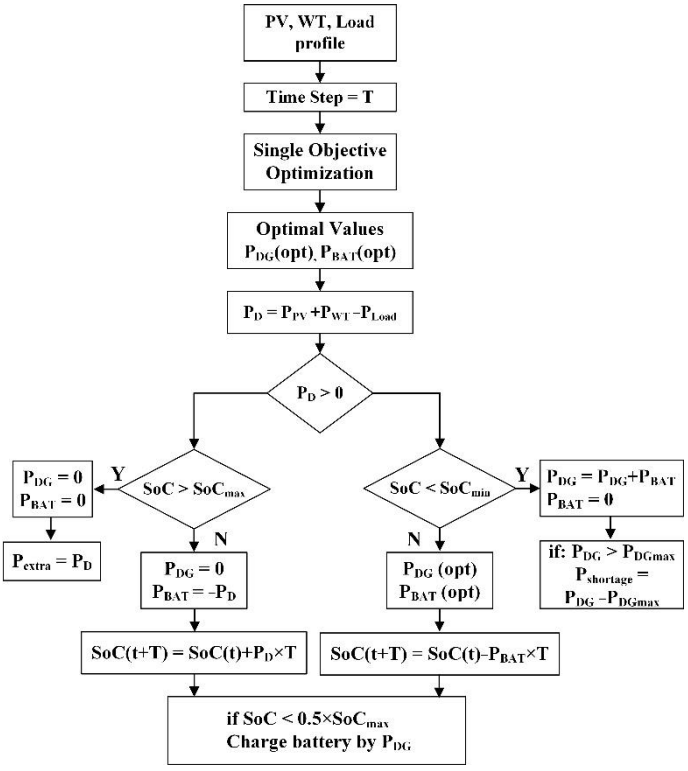

Figure 3. Power management algorithm for the HIMG.

As it can be seen from Figure 4, according to the power amounts of PV, WT, and Load at each time step, a single-objective optimization was employed to obtain the optimal values for DG and BAT considering the constraints in (4)–(7). If the REs meet the load, this difference power (PD) can charge the battery if the battery is not fully charged. On the contrary, if the battery is fully charged (SoCmax), then PD identifies as extra power. In this case, DG is not necessary to produce power to provide the power balance. On the other hand, if the REs are insufficient to supply the load, the DG and BAT participate economically to provide the required power for the load. In this case, the battery discharges if a portion of load demand is supplied by battery power. Supplementary battery management is also provided to check the SoC battery in each iteration. By evaluating the possibility of DG generation, the battery can be charged at least at the level of 50%.

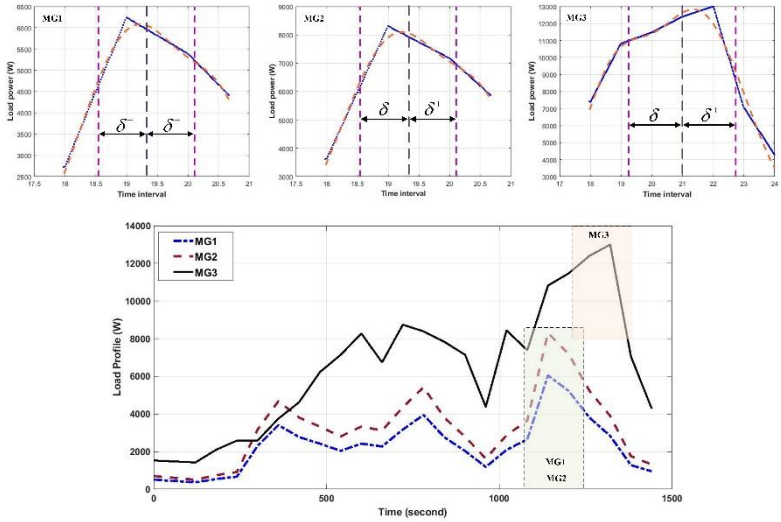

Figure 4. Load profile for each MG of the NMG.

Particle swarm optimization (PSO) was utilized in this paper as a single-objective optimization. However, other algorithms, such as differential evolution (DE), genetic algorithm (GA), and imperialist competitive algorithm (ICA), are also able to deal with this problem. PSO represents a robust, rapid, and reliable performance among different optimization algorithms. In the PSO algorithm, the particles are identified by position and velocity. At the initial phase, the particles position and particle best position are initialized. Then, over the iterations, the particles' position and velocity are updated to propel the particles toward the global best [25].

2.3. Evaluation of the HIMG Operation (RF Calculation)

According to the optimal operation of the HIMG, the optimal produced energy of the energy generator units and consequently the OR of MGs can be calculated over a specific interval. Interactive transfer or receiving energy in the MG community results in higher OR in MGs. Therefore, optimal component sizing in the NMG can effectively reduce MGs' capital, replacement, and M&O cost. The reduced factor proposed in this section was based on two main factors, the PL and correlation of load profile. Due to the dependency of the proposed RF to the OR of MGs, the RF affects the dispatchable components of the MGs. The RF is expressed in (9):

$$RF_{MG_i} = \frac{\left[OR_{MG_i} \times \frac{OC_{MG_i} - PL}{OC_{MG_i}}\right]_{MG_i}^{\|\delta_i^- - \delta_i^+\|} \times \left(2 - \prod_{j=1}^{N} corr(MG_i, MG_j)\right)}{\left[OR_{MG_i} \times \frac{OC_{MG_i} - PL}{OC_{MG_i}}\right]_{MG_i}^{\|\delta_i^- - \delta_i^+\|} + \frac{1}{N-1} \sum_{\substack{j=1 \\ j \neq i}}^{N} \left[OR_{MG_j} \times \frac{OC_{MG_j} - L_{\max}}{OC_{MG_j}}\right]_{MG_j}^{\|\delta_i^- - \delta_i^+\|}} \quad (9)$$

In (9), $||\delta^+ - \delta^-||$ represents the interval at which *PL* occurs, at $(\delta^+ + \delta^-)/2$, and the OR of other MGs are also calculated in this interval; therefore, only PL and the maximum load profile (L_{max}) are identical if the load patterns are similar. For instant, when the MG_1 and MG_2 are at PL, the MG_3 is not in its PL. In addition, N is the number of MGs that existed in the NHMG, and *corr* represents the correlation of the load pattern among MGs. The Pearson's linear correlation coefficient was utilized to evaluate the correlation of the Load profile:

$$corr(MG_i,\ MG_j) = \frac{\sum_{k=1}^{n} (MG_{i,k} - \overline{MG_i})(MG_{j,k} - \overline{MG_j})}{\left\{ \sum_{k=1}^{n} (MG_{i,k} - \overline{MG_i})^2 \sum_{l=1}^{n} (MG_{j,k} - \overline{MG_j}) \right\}^{\frac{1}{2}}} \quad (10)$$

where $\overline{MG}$ is the mean value of n data of MG's load profile. This correlation coefficient returns a value between -1 and 1, if a perfect negative correlation and perfect positive correlation exists among the data, respectively. To obtain the δ for MGs, a Gaussian curve with a mean (μ) of PL ($\mu = PL$) was fitted to the load profile. The standard deviation of the fitted curve was considered as δ. Figure 4 demonstrates the Gaussian fitted curve to the MG load profiles. The following results can be deduced from (9):

- The calculations were based on the OR of a specific MG during the PL in the interval $||\delta^+ - \delta^-||$. This time interval is considered for the other MGs that exist in the NHMG. The ORs were calculated based on the optimal operation of HIMGs.
- The ORs are given importance by the factor of *PL* and *OC* difference. Therefore, the higher PL led to reducing lower OR in the NMG in order to increase the MG reliability.
- The correlation represents the PL coincidence of MGs. Therefore, the correlation with a value that is lower than the unity resulted in a higher RF due to the possibility of sharing OR of adjacent MGs.

3. Evaluation and Simulation Results

According to the optimal design of the HIMG with HOMER and the discussed power management algorithm in Figure 4, the ORs of HIMGs were calculated. To this end, the simulation was conducted in MATLAB. Eventually, according to Equation (9), the *RF*s were calculated in order to obtain the optimal design in the NHMG. Figure 5 shows the optimal operation of the HIMGs. The SoC of the batteries and extra and shortage power are also presented in Figure 5. The initial SoC of the batteries was set to 50%, and as can be observed, the extra power leads to charging the batteries completely.

The simulation was performed for 24 h, and the time step was set to 15 min to reduce the large quantity of data produced. The ORs were calculated for two different intervals $||\delta^+ - \delta^-||$. The PL of MG_1 and MG_2 is a coincidence at the same time, and the OR for MG_3 was also calculated during the PL of two other MGs. Furthermore, the OR during the PL of MG_3 was calculated for MG_1 and MG_2 to obtain the RF of MG_3. To evaluate the battery power, the C-rate was considered as 5C. The correlation was calculated by using *the* "*corr*" function in MATLAB. The load profile of MG_1 and MG_2 are similar with different scales. Therefore, the correlation for these two MGs is unity. However, the correlation between MG_1 and MG_3 was obtained as 0.8727. Table 5 presents the HIMG specifications and *RFs* for the HIMGs. The RF represents the OR reduction percentage in each HIMG when the MGs are in collaborative operation as the NHMG. Therefore, in order to evaluate the optimal component size for the HNMG, the reduced power generation units were obtained as follows:

$$\min\{\alpha \times CF(DG) + \beta \times CF(BAT)\} \quad (11)$$

Subject to:

$$P_{MG_i}^{DG} + P_{MG_i}^{BAT} = \frac{RF_{MG_i} \times OR_{MG_i}}{\|\delta_i^- - \delta_i^+\|} \quad (12)$$

where DG and battery cost functions are defined in Table 1, and α and β weighed the priority of DG and battery cost functions, respectively. The reduced OR for MGs over the time interval $||\delta^{+} - \delta^{-}||$ represents the amount of power. Eventually, the optimum result of DG and battery power from the minimization problem in (11) was deduced from the optimum results obtained from the algorithm in Figure 4. Due to the high M&O cost and the lower lifetime of batteries to produce energy, β was considered a higher value in this research in order to decrease the size of the more compared with DG. The optimum size of DG and batteries according to the proposed algorithm is presented in Table 5.

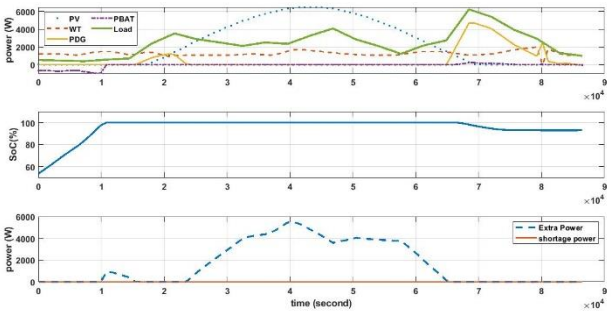

(**a**): MG_1

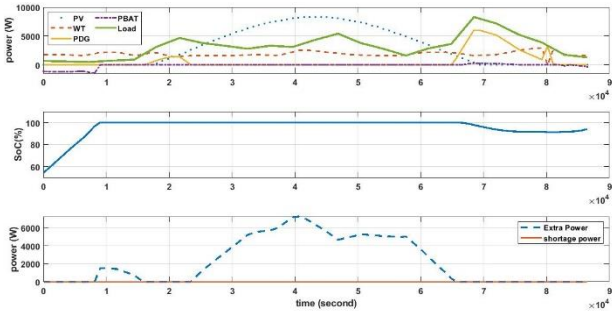

(**b**): MG_2

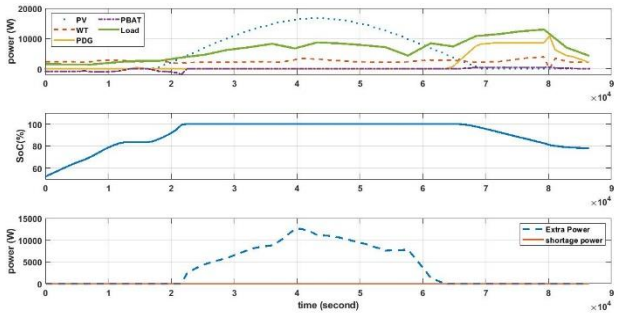

(**c**): MG_3

Figure 5. Optimal operation of the HIMGs: (**a**) MG_1, (**b**) MG_2, and (**c**) MG_3.

Table 5. HIMG specifications.

	PGU	MG1	MG2	MG3	Total
OR (kWh) for MG_1 and MG_2	DG	4.4	6.45	13.44	24.29
	BAT	9.64	12.73	19.04	41.41
OR (kWh) for MG_3	DG	13.57	19.16	19.31	52.04
	BAT	14.92	19.79	28.56	63.27
OC (kW)	DG	6.8	9.1	15	30.9
	BAT	5.8	7.6	11.4	24.8
Peak Load (kW)		6.2	8.3	13	27.5
Electric Load (EL) (kWh/day)		237.83	316.49	630.46	1184.78
Unmet load (kWh/day)		0	0	0	0
Extra power (kWh/day)		160.02	216.99	351.73	728.74
RF (%)		41	52	68	-
DG (kW)		3.8	4.8	8.2	-
BAT (kW)		3.2	3.8	6.4	-

4. Verification of the Results in the NHMG

To verify the results of the optimal and economical sizing components in an NMG, according to the calculated RF in Table 5, an algorithm to control the NHMG is proposed. The optimum operation of the NHMG was evaluated considering the hybrid control strategy defined in Figure 6. Hybrid control refers to the control strategies that take advantage of both centralized and decentralized control strategies. The centralized controller is applied in order to obtain the optimal operation of each HIMG. On the other hand, the decentralized controller is responsible for the optimum operation of the whole system by knowing the essential data from the centralized controller. As it can be observed from Figure 6, multi-objective optimization was utilized in the algorithm as a centralized controller for each HIMG.

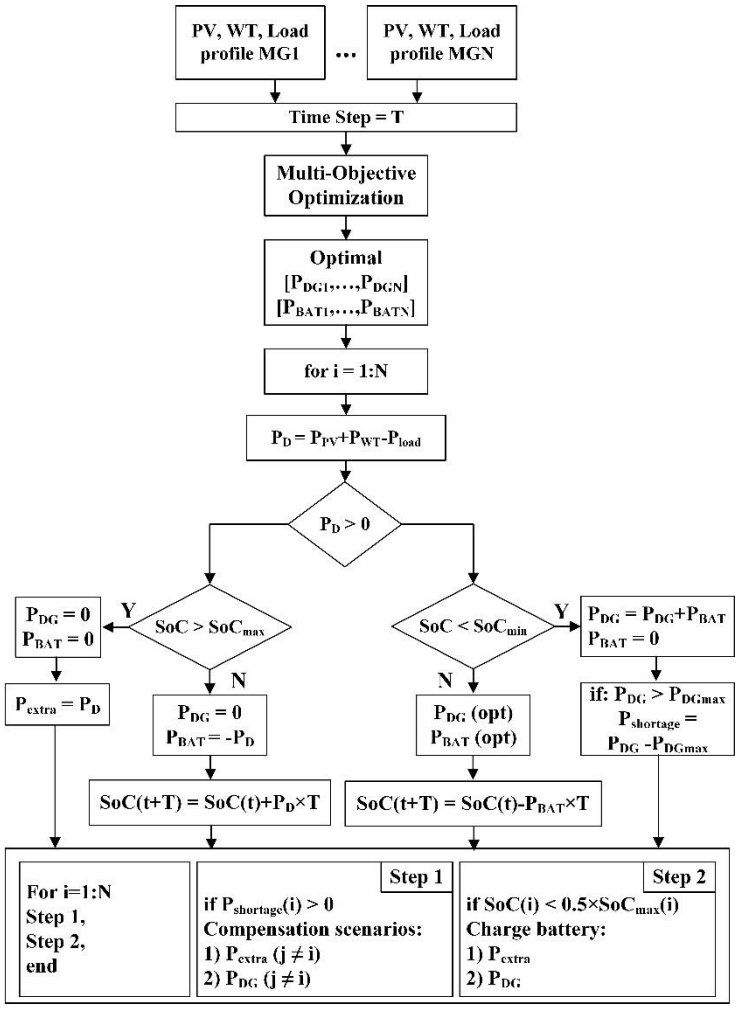

Figure 6. Hybrid control strategy in the NHMG.

The multi-objective optimization was implemented with the MOPSO and PESA-II algorithms in order to establish a comparison between these two optimization methods. MOPSO and PESA-II are technically similar. However, in PESA-II, the PSO algorithm is replaced with GA. In multi-objective optimization problems, the proposed algorithms utilize different methods to discover the non-dominated solutions and produce the Pareto frontier. The non-dominated solutions were produced using the concept of dominance in MOPSO and PESA-II. Moreover, both of the afore-mentioned optimization methods have region-based selection in leader and objective space in order to improve the diversity of the Pareto frontier [25].

Then, the essential information, i.e., DG and battery power, was obtained from the decentralized controller to provide an optimal operation for the NHMG. Compared with

the HIMG algorithm, a supplementary control to check the possibility of power sharing amongst MGs was applied to the algorithm in Figure 6. In this case, the extra power and shortage power can effectively interact through the MGs to have a reliable operation. To this end, two complementary steps were considered in order to take advantage of power sharing in the NHMG. At the first step, the MG with a power shortage attempts to meet the load first by the extra energy from other MGs, and if the extra energy does not existed or is sufficient to meet the power shortage, the DGs in MGs can assist by supplying the load completely. Moreover, in step 2, the SoC of the batteries check if they need charging if the SoC is less than 50% and extra energy and DG power exist to charge the batteries.

4.1. Simulation Results

In order to evaluate the operation of the NHMG by considering the sizing component design procedure in Section 3, the simulation was conducted according to the control algorithm in Figure 6. Two multi-objective optimization methods were implemented in MATLAB to optimize the operation of each HIMG, and the supplementary control was exploited to optimize the operation of the entire system. The multi-objective optimization proposed a set of optimal solutions as a Pareto frontier. To choose the proper solution, several methods can be applied to the problem. The evaluation of the solutions, feature selection, and clustering methods are usual methods to select a single or multi solution amongst several Pareto solutions.

In this simulation, k-means were applied to the problem to select the center of the cluster using Lloyd's algorithm as a proper solution among the produced Pareto set. In Figure 7, the operation of the NHMG by MOPSO optimization is demonstrated. Moreover, Table 6 is provided in order to compare the obtained results from the two optimization algorithms.

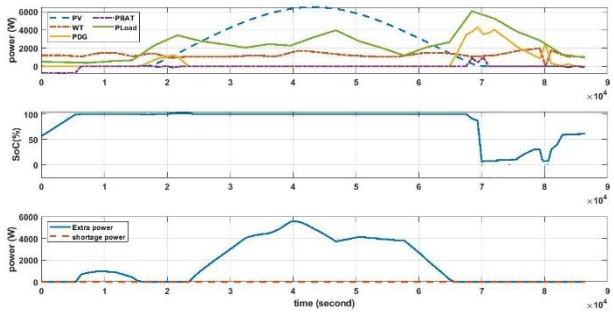

(**a**): MG_1

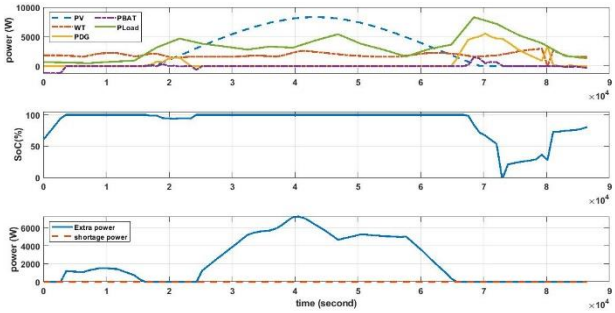

(**b**): MG_2

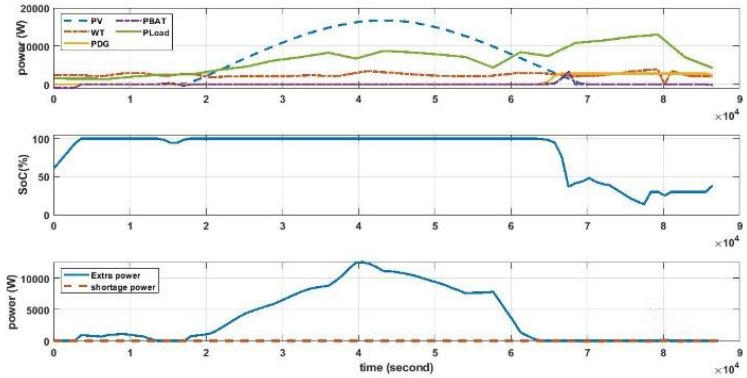

(**c**): MG_3

Figure 7. Optimal operation of the HNMGs: (**a**) MG_1, (**b**) MG_2, and (**c**) MG_3.

Table 6. Optimal operation of the NHMG.

		MOPSO			PESA-II		
	PGU	**MG_1**	**MG_2**	**MG_3**	**MG_1**	**MG_2**	**MG_3**
OR (kWh/day) for MG_1 and MG_2	DG	4.40	6.45	13.44	4.54	6.75	13.76
	BAT	9.64	12.73	19.04	9.50	12.43	18.84
OR (kWh/day) for MG_3	DG	13.57	19.16	19.31	13.87	19.36	19.50
	BAT	14.92	19.79	28.56	14.62	19.59	28.22
Unmet load (kWh/day)		0	0	0	0	0	0
Extra power (kWh/day)		160.02	216.99	351.73	159.74	216.55	350.66

To compare the performance of the two optimization algorithms, the simulation was conducted in one laptop set. The results obtained from PESA-II are slightly more accurate due to providing a more optimal solution. However, the performance of PESA-II is slower than that of MOPSO (about 8 min for MOPSO vs. 28 min for PESA-II). In addition, the initial parameters related to the PESA-II were more sensitive in order to be adjusted accurately.

4.2. Practical Results

The experiments were implemented using a GPiB communication protocol, and RS485 Modbus transmits the measured values. Figure 8 shows the implemented structure of the NHMG. To achieve the performance of the batteries and WT energy, the optimal results of the central controller affect the load profile. The solar radiation profile was applied to the solar array simulator (SAS) to emulate solar energy. Furthermore, it is essential to define the short circuit current (*Isc*), maximum power point current (*Impp*), open-circuit voltage (*Voc*), and maximum power point voltage (*Vmpp*) of the solar panel for SAS:

$$I_{sc} = I_{sc}^{ref} \times \left(\frac{G}{G_{ref}} \right) \tag{13}$$

$$I_{mpp} = I_{mpp}^{ref} \times \left(\frac{G}{G_{ref}} \right) \tag{14}$$

$$V_{oc} = V_{oc}^{ref} + \alpha \ln \left(\frac{G}{G_{ref}} \right) \tag{15}$$

$$V_{mpp} = V_{mpp}^{ref} - \beta \left(T_{ref} - T \right) \tag{16}$$

where G is the solar radiation (W/m^2), α is modified ideality factor ($\alpha = K \times Temp/q$, where K is the Boltzmann constant, $Temp$ is cell temperature, and q is electron charge), and β is the temperature coefficient. The temperature is considered constant, $T = Tref$. Figure 9 shows the laboratory experiments' configuration of the three MGs. Figure 10 represents the optimal operation of the NMG according to the reduced component sizing calculated by the proposed algorithm. As can be observed, the produced energy by the power generator units can meet the load effectively.

As can be observed from Figure 10, the load is met by power generation units effectively, and the surplus energy is transferred to the main grid through the grid-connected inverter. The grid-connected inverter used in the laboratory has a 30 s delay in order to start working in synchronization with the main grid. This delay can be seen in the PV power generation graph in Figure 10.

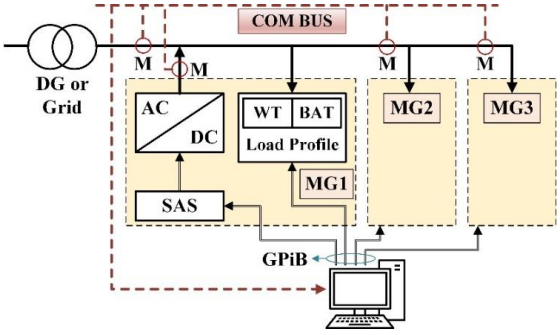

Figure 8. Implemented structure of the NHMG.

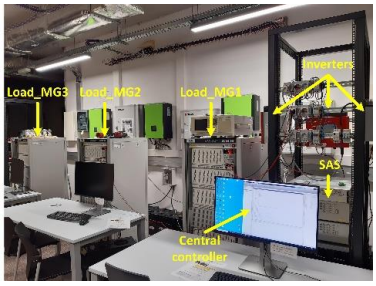

Figure 9. Laboratory experiments' configuration.

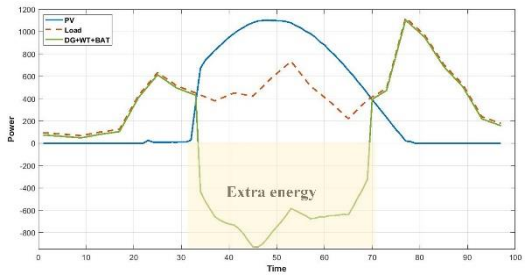

(**a**)

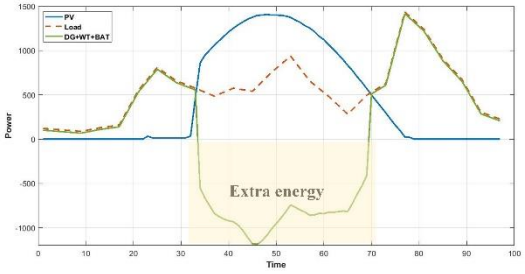

(**b**)

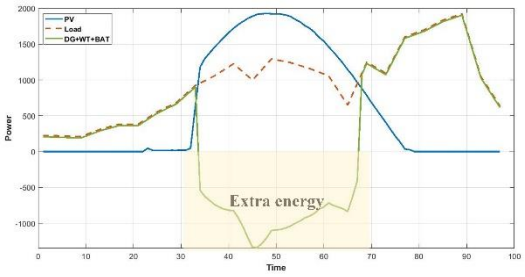

(**c**)

Figure 10. Practical results of the HIMGs: (**a**) MG_1, (**b**) MG_2, and (**c**) MG_3.

5. Conclusions

A component sizing procedure for a NHMG was proposed in this paper. The proposed algorithm was based on the OR and peak loads of MGs. To this end, the optimal operation of HIMGs was evaluated to obtain the optimal OR of each MG. Consequently, a reduced factor (RF) was presented in order to reduce the dispatchable component size of MGs. The RF was based on the OR, the peak load, and the correlation of load pattern. Therefore, NHMGs with different load patterns resulted in an RF increase and component size decrease. Due to the possibility of power sharing in NHMGs, the proposed algorithm did not affect the reliability of MGs by reducing the OR. The simulation results for the NHMG by using two different multi-objective optimizations, i.e., MOPSO and PESA-II, were analyzed. The results show that, in the NHMG, the size of the dispatchable generation units can decrease effectively. Therefore, the capital, operational, and M&O cost of the MGs can be reduced significantly. Finally, the results of the laboratory experiments were presented in order to verify the proposed algorithm.

Author Contributions: Conceptualization, N.S.; methodology, N.S. and H.M.-G.; software, N.S.; validation, N.S., H.M.-G. and G.V.-Q.; investigation, N.S.; data curation, N.S. and H.M.-G.; writing—original draft preparation, N.S. and H.M.-G.; writing—review and editing, N.S., H.M.-G. and G.V.-Q.; supervision, H.M.-G. and G.V.-Q. All authors have read and agreed to the published version of the manuscript.

Funding: Grant PGC2018-098946-B-I00, funded by: MCIN/AEI/10.13039/501100011033/and by ERDF A way of making Europe.

Institutional Review Board Statement: Not applicable.

Informed Consent Statement: Not applicable.

Data Availability Statement: Not applicable.

Acknowledgments: The authors would like to thank the Spanish Ministerio de Ciencia, Innovación y Universidades (MICINN)—Agencia Estatal de Investigación (AEI) and the European Regional Development Funds (ERDF) by grant PGC2018-098946-B-I00 funded by MCIN/AEI/10.13039/501100011033/ and by ERDF A way of making Europe.

Conflicts of Interest: The authors declare no conflict of interest.

Nomenclature

CC	Cycling Charging
CF	Cost Function
COE	Cost of Electricity
DE	Differential Evolution
DER	Distributed Energy Resources
DG	Diesel Generator
DSM	Demand-Side Management
EMS	Energy Management System
ESS	Energy Storage System
EV	Electric Vehicle
GA	Genetic Algorithm
HIMG	Hybrid Individual Microgrid
HMG	Hybrid Microgrid
ICA	Imperialist Competitive Algorithm
IMG	Individual Microgrid
LCC	Life-Cycle Cost
LCE	Levelized Cost of Energy
LF	Load Following
LLP	Loss-of-Load Probability
LPSP	Loss-of-Power Supply Probability
MADE	Mutation Adaptive Differential Evolution

MG	Microgrid
MOEA/D	Multi-Objective Evolutionary Algorithm Based on Decomposition
MOSaDE	Multi-Objective Self-Adaptive Differential Evolution
MOPSO	Multi-Objective Particle Swarm Optimization
MPPT	Maximum Power Point Tracking
NHMG	Networked Hybrid Microgrid
NMG	Networked Microgrid
NPC	Net Present Cost
NTC	Net Total Cost
OC	Operating Capacity
OR	Operating Reserve
PE	Produced Energy
PESA-II	Pareto Envelop-based Selection Algorithm II
PL	Peak Load
PV	Photovoltaic
RE	Renewable Energy
RES	Renewable Energy Source
RF	Reduced Factor
SAS	Solar Array Simulator
SoC	State of Charge
SPEA-II	Strength Pareto Evolutionary Algorithm II
SAPV	Stand-Alone PV
WT	Wind Turbine

References

1. Kumar, P.S.; Chandrasena, R.P.S.; Ramu, V.; Srinivas, G.N.; Babu, K.V.S.M. Energy Management System for Small Scale Hybrid Wind Solar Battery Based Microgrid. *IEEE Access* **2020**, *8*, 8336–8345. [CrossRef]
2. Mohammed, K.; Mohammed, O.H.; Alshammari, N.; Akherraz, M. Multi-objective optimization and the effect of the economic factors on the design of the microgrid hybrid system. *Sustain. Cities Soc.* **2021**, *65*, 102646.
3. Ramli Makbul, A.M.; Bouchekara, H.R.E.H.; Alghamdi, A.S. Optimal sizing of PV/wind/diesel hybrid microgrid system using multi-objective self-adaptive differential evolution algorithm. *Renew. Energy* **2018**, *121*, 400–411. [CrossRef]
4. Mohammed, R.H.; Gomes, C.; Hazim, H.; Ahmadipour, M. Sizing and implementing off-grid stand-alone photovoltaic/battery systems based on multi-objective optimization and techno-economic (MADE) analysis. *Energy* **2020**, *207*, 118163.
5. Bouchekara, H.R.E.-H.; Javaid, M.S.; Shaaban, Y.A.; Shahriar, M.S.; Ramli, M.A.M.; Latreche, Y. Decomposition based multiobjective evolutionary algorithm for PV/Wind/Diesel Hybrid Microgrid System design considering load uncertainty. *Energy Rep.* **2020**, *7*, 52–69. [CrossRef]
6. Ridha, H.M.; Gomes, C.; Hizam, H.; Ahmadipour, M.; Muhsen, D.H.; Ethaib, S. Optimum Design of a Standalone Solar Photovoltaic System Based on Novel Integration of Iterative-PESA-II and AHP-VIKOR Methods. *Processes* **2020**, *8*, 367. [CrossRef]
7. Anderson Alexander, A.; Suryanarayanan, S. Review of energy management and planning of islanded microgrids. *CSEE J. Power Energy Syst.* **2019**, *6*, 329–343.
8. Wei, F.; Jin, M.; Liu, X.; Bao, Y.; Marnay, C.; Yao, C.; Yu, J. A review of microgrid development in the United States—A decade of progress on policies, demonstrations, controls, and software tools. *Appl. Energy* **2018**, *228*, 1656–1668.
9. Vinny, M.; Adetunji, K.E.; Joseph, M.K. Planning of a sustainable microgrid system using HOMER software. In Proceedings of the 2020 Conference on Information Communications Technology and Society (ICTAS), Durban, South Africa, 11–12 March 2020; pp. 1–5.
10. Zahid, J.; Li, K.; Hassan, R.U.; Chen, J. Hybrid-microgrid planning, sizing and optimization for an industrial demand in Pakistan. *Teh. Vjesn.* **2020**, *27*, 781–792.
11. Wencong, S.; Yuan, Z.; Chow, M. Microgrid planning and operation: Solar energy and wind energy. In Proceedings of the IEEE PES General Meeting, Providence, RI, USA, 25–29 July 2010; pp. 1–7.
12. Yu, P.; Liu, L.; Zhu, T.; Zhang, T.; Zhang, J. Feasibility analysis on distributed energy system of Chongming County based on RETScreen software. *Energy* **2017**, *130*, 298–306.
13. Gasparovic, G.; Krajačić, G.; Duić, N.; Baotić, M. New Energy Planning Software for Analysis of Island Energy Systems and Microgrid Operations – H2RES Software as a Tool to 100% Renewable Energy System. *Comput. Aid. Chem. Eng.* **2014**, *33*, 855–1860.
14. Michalitsakos, P.; Mihet-Popa, L.; Xydis, G. A Hybrid RES Distributed Generation System for Autonomous Islands: A DER-CAM and Storage-Based Economic and Optimal Dispatch Analysis. *Sustainability* **2017**, *9*, 2010. [CrossRef]
15. Essiet, I.O.; Sun, Y.; Wang, Z. Analysis of the Effect of Parameter Variation on a Dynamic Cost Function for Distributed Energy Resources: A DER-CAM Case Study. *Appl. Sci.* **2018**, *8*, 884. [CrossRef]

16. Comodi, G.; Cioccolanti, L.; Gargiulo, M. Municipal scale scenario: Analysis of an Italian seaside town with MarkAL-TIMES. *Energy Policy* **2012**, *41*, 303–315. [CrossRef]
17. Zia Muhammad, F.; Benbouzid, M.; Elbouchikhi, E.; Muyeen, S.M.; Techato, K.; Guerrero, J.M. Microgrid transactive energy: Review, architectures, distributed ledger technologies, and market analysis. *IEEE Access* **2020**, *8*, 19410–19432.
18. Islam, M.; Yang, F.; Amin, M. Control and optimisation of networked microgrids: A review. *IET Renew. Power Gener.* **2021**, *15*, 1133–1148. [CrossRef]
19. Yi, W.; Rousis, A.O.; Strbac, G. A Three-Level Planning Model for Optimal Sizing of Networked Microgrids Considering a Trade-Off Between Resilience and Cost. *IEEE Trans. Power Syst.* **2021**, *36*, 5657–5669.
20. Afolabi, Y.A.; AlMuhaini, M.; Heydt, G.T. Optimal design of hybrid DG systems for microgrid reliability enhancement. *IET Gener. Transm. Distrib.* **2020**, *14*, 815–823.
21. Hakimi, S.M.; Hasankhani, A.; Shafie-Khah, M.; Lotfi, M.; Catalão, J.P. Optimal sizing of renewable energy systems in a Microgrid considering electricity market interaction and reliability analysis. *Electr. Power Syst. Res.* **2021**, *203*, 107678. [CrossRef]
22. Hakimi, S.M.; Hasankhani, A.; Shafie-Khah, M.; Catalão, J.P. Optimal sizing and siting of smart microgrid components under high renewables penetration considering demand response. *IET Renew. Power Gener.* **2019**, *13*, 1809–1822. [CrossRef]
23. Moslem, U.; Romlie, M.F.; Abdullah, M.F.; Halim, S.A.; Kwang, T.C. A review on peak load shaving strategies. *Renew. Sustain. Energy Rev.* **2018**, *82*, 3323–3332.
24. Norberto, F.; Sanz, Y.; Rodrigues, M.; Montañés, C.; Dopazo, C. The use of cost-generation curves for the analysis of wind electricity costs in Spain. *Appl. Energy* **2011**, *88*, 733–740.
25. Navid, S.; Martinez-Garcia, H.; Velasco-Quesada, G.; Guerrero, J.M. A Comprehensive Review of Control Strategies and Optimization Methods for Individual and Community Microgrids. *IEEE Access* **2022**, *10*, 15935–15955.